การประชุมวิชาการเครือข่ายวิศวกรรมเครื่องกลแห่งประเทศไทยครั้งที่ 18
18-20 ตุลาคม 2547 จังหวัด-ขอนแก่น

On the Optimum Handling and Vibration Control of an Electrohydraulic Active Suspension with Pole-Assignment Technique

ประกอบ สุรวัฒนาวรรณ
ภาควิชาวิศวกรรมเครื่องกล คณะวิศวกรรมศาสตร์ มหาวิทยาลัยเกษตรศาสตร์ 50 ถนนพหลโยธิน เขตจตุจักร กรุงเทพฯ 10900
โทร 02-9428555 ต่อ1802 โทรสาร 02-5794576 Email:fengpsw@ku.ac.th
Prakob Surawattanawan
Department of Mechanical Engineering, Faculty of Engineering, Kasetsart University, 50 Phaholyothin Rd, Bangkok 10900, Thailand
Tel: 02-9428555 ext.1802 Fax: 02-5794576 Email:fengpsw@ku.ac.th

Abstract

Electrohydraulic active suspensions have recently attracted increased attention in automobile industry because they can significantly improve the compromise between many conflicting ride and handling measures of vehicle performance. Ideal hydraulic force models have been used in active suspension studies for decades. However, few studies have included hydraulic effects, which are the core of system force generator, in the controller design due to its complexities. In this paper a novel approach is presented to incorporate hydraulic components in the modeling and controller design stage. The method of state-space modeling and pole-assignment technique are applied in order to determine the optimum solution for the minimization of car body acceleration as well as other outputs representing handling quality and design constraints. Comparisons between optimum Passive Suspension (PS) and optimum Active Suspension designed by Pole-Assignment technique (ASPA) have been made. Results show that the trend of the carpet plots for the ASPA is similar to that of the PS. For each system natural frequency, there is an optimum damping level at which the car body acceleration level is minimised. This is due to the fact that the dominant natural frequency and damping ratio in the ASPA are equivalent to the suspension stiffness and damping rate in the PS. The optimum solution of the ASPA occurs at the lowest system natural frequency and the limitation is the control stability. It is found that the ASPA, designed by the system natural frequencies lower than 1.6 Hz, will become unstable. Regarding magnitude responses, there is no difference for the tire deflections or vehicle handling between both optimum designs. The ASAP is superior to the PS with respect to the minimization of vibration. The ASPA can reduce the vibration level to 51% of that obtained from the PS whilst the ASPA utilises less suspension displacement than the PS 12%. Even though the ASPA provides the better performance in comparison to the PS, the conceptual designs of both are similar. The optimum designs are still the trade-off between the effects of transmissibility and system natural frequency.

Key-words: automotive active suspension, electrohydraulic system, state-space modeling, pole-assignment control

Nomenclature

- A_c actuator cross-sectional area = 2.46 x 10^{-4} m^2
- B_t tire damping rate = 4000 N/m s^{-1}
- B_v actuator viscous damping rate = 300 N/m s^{-1}
- e control signal
- F hydraulic force (N)
- G D/A gain = 6.25 x 10^{-3} mA/PSCno.
- i applied current to servovalve (mA)
- i_0 applied current to servovalve at steady-state (mA)
- k_f flow constant of servovalve = 7.38 x 10^{-9} m^3 s^{-1}/mA $(N\ m^{-2})^{1/2}$
- k_i flow gain of servovalve = 2.3 x 10^{-5} m^3 s^{-1}/mA
- k_{i1} flow gain for side 1 of servovalve (m^3 s^{-1}/mA)
- k_{i2} flow gain for side 2 of servovalve (m^3 s^{-1}/mA)
- k_{P1} pressure gain for side 1 of servovalve (m^3 s^{-1}/N m^{-2})
- k_{P2} pressure gain for side 2 of servovalve (m^3 s^{-1}/N m^{-2})
- k_t tire stiffness = 2.8 x 10^5 N/m
- m wheel unit mass = 40 kg
- M car body mass = 240 kg
- N A/D gain = 1600 PSCno./V
- P forward gain for a controller = 0.85
- P_1 pressure for side 1 of actuator (N/m^2)
- P_2 pressure for side 2 of actuator (N/m^2)
- P_S supply pressure = 200 bar
- P_{10} pressure for side 1 of actuator at steady state = 148 bar
- P_{20} pressure for side 2 of actuator at steady state = 52 bar
- Q flow rate (m^3/s)
- Q_1 flow rate for side 1 of actuator (m^3/s)
- Q_2 flow rate for side 2 of actuator (m^3/s)

Q_i input flow rate (m^3/s)

Q_o output flow rate (m^3/s)

R_i internal leakage resistance = 98 x 10^9 N m^{-2}/m^3 s^{-1}

V actuator chamber and hose volume = 7.13 x 10^{-5} m^3

V_1 V for side 1 of actuator (m^3)

V_2 V for side 2 of actuator (m^3)

z_b car body displacement (m)

z_w wheel hub displacement (m)

z_r road input displacement (m)

$z_b - z_w$ suspension displacement (m)

$z_r - z_w$ tire deflection (m)

β_e effective bulk modulus = 0.22 x 10^9 N/m^2

α actuator angle = 27 °

ζ damping ratio

ω_n undamped natural frequency (rad/s)

I_1 gain for car body velocity sensor = 5 V/ms^{-1}

F_1 gain for suspension displacement sensor = 57.2 V/m

J_1 gain for wheel velocity sensor = 5 V/ms^{-1}

H_1 gain for load cell sensor = 66.7x10^{-6} V/N

L_1 gain for tire deflection sensor = 18.18 V/m

I_2 feedback gain for car body velocity = 0.244

F_2 feedback gain for suspension displacement = 0.0064

J_2 feedback gain for wheel velocity = 0.277

H_2 feedback gain for hydraulic force = -2.602

L_2 feedback gain for tire deflection = 0.356

1. Introduction

The possible applications of eletrohydraulic active suspension range from ride/handling control of automotive vehicles, to maneuverability of tanks and off-road vehicles and superior ride height and stability control of champion ship race car [1,4]. The potential of eletrohydraulic active suspension have been assessed with the assistance of the control theory since the early 1980s [8]. The first attempt on hydraulic modeling was investigated by Mrad *et al* [10]. A Non-linear model of hydraulic components was presented along with simulation results. The support spring was placed in parallel with the hydraulic actuator. Actuator viscous damping and actuator oil leakage were neglected and there was no discussion about how to utilise the non-linear model for the controller design.

Engelman and Rizzoni [6] studied a model that includes non-linear servovalve equations and proposed a linearization technique to obtain linear equations. However, there were two questions arising in this paper. Firstly, the assumption of operating condition (supply pressure, pressures at both servovalve ports, and tank return pressure) was not defined. As a result it was not possible to obtain linearized gains, and a linear model analysis could not be investigated. Secondly, there was no information of constant parameters used for simulation. Therefore, the simulation results and discussion is in question. From the viewpoint of modeling, a spring was placed in parallel with the actuator, therefore instability does not occur. Moreover, the model neglected actuator viscous damping and actuator oil leakage.

Thompson and Chaplin [15] also proposed a hydraulic actuator placed in parallel with a support spring. Their model neglected tire damping, actuator viscous damping, and actuator oil leakage. Their analysis began from non-linear servovalve equations which were processed into two cases separately (extending and retracting cases). Numerical constants were provided based on an assumption. The system operating condition was well defined. The analysis finished with two non-linear equations representing both directional movements of the actuator. The non-linear model was inserted into a linear quarter car model by block diagram analysis. Simulation was used to demonstrate a different response to road input for active suspensions with and without the hydraulic model. It should be noted that Thompson and Chaplin were not able to include the non-linear hydraulic model during the controller design stage due to nonlinear servovalve model.

An important task for active suspension design is the determination of parameters in a control law that is capable of giving good system performance. The control law replaces a spring stiffness and a damper coefficient and typically more parameters than the passive system possesses are involved. Also, the parameter values are less constrained. Although many different forms of control designs have been proposed, attention here will be confined to fixed-gain full-state feedback control schemes, namely pole-assignment control (PA).

Even though the PA is a standard method to obtain a full-state feedback controller, few studies have applied this method to the active suspension. This research has been found only one notable publication, that of Hall and Gill [7]. Skyhook damping arrangement was applied and Ideal force model was used. Hydraulic model and tire damping were neglected. Absolute displacements of car body and wheel unit were used for state feedback. This was impossible for physical realization. Hall and Gill examined the effects of closed-loop pole locations on the performance of the active suspension and attempted to find an optimum design solution. The closed-loop poles were varied according to the locations in s-plane and each configuration was

used to plot transmissibility relating road input velocity to wheel and car body velocities. An optimum design was considered from the transmissibility, which is close to the ideal one. The work of Hall and Gill encouraged the further development in this research work.

Most of foregoing works have developed active suspension controls on the basis of an idealized hydraulic actuator capable of delivering force infinitely fast. However, obtaining high fidelity actuation in practice is a very challenging task requiring full understanding of hydraulic system dynamics. Therefore, the issue of the connection between actuator dynamics and controller design becomes another important aspect of practical significance for active suspension control.

The objective of this work is to incorporate hydraulic components in the controller design stage. The method of pole-assignment is applied in order to determine the optimum solution for ride comfort (the minimization of car body acceleration) and road holding (the minimization of tire deflection) within the physical constraint (suspension stroke). Comparisons between optimum Passive Suspension (PS) and optimum Active Suspension designed by Pole-Assignment technique (ASPA) have been made. Consider the configuration of electrohydraulic active suspension in Fig 1

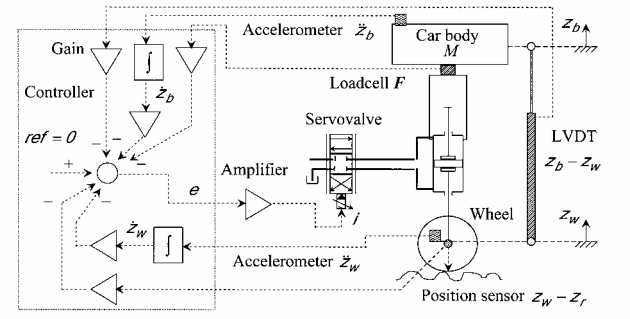

Fig 1 Electrohydraulic active suspension model [14]

It comprises a high pressure hydraulic actuator in place of a conventional spring and shock absorber, and a servovalve used to control hydraulic flow rate to the actuator. The model of eletrohydraulic active suspension including hydraulic terms can be written in state-space format [2,17] as follows:-

$$\dot{\mathbf{x}} = \mathbf{A}\mathbf{x} + \mathbf{B}e + \mathbf{G}_\mathbf{d}\dot{z}_r \qquad (1)$$

where

$\mathbf{x}$ = state vector = $\begin{bmatrix} \dot{z}_b \\ \dot{z}_w \\ F \\ z_b - z_w \\ z_w - z_r \end{bmatrix}$

$\mathbf{A}$ = system matrix = $\begin{bmatrix} -\frac{B_v}{M} & \frac{B_v}{M} & \frac{\cos\alpha}{M} & 0 & 0 \\ \frac{B_v}{m} & -\frac{(B_v + B_t)}{m} & -\frac{\cos\alpha}{m} & 0 & -\frac{k_t}{m} \\ -\frac{2\beta_e A_c^2}{V} & \frac{2\beta_e A_c^2}{V} & -\frac{2\beta_e}{VR_i} & 0 & 0 \\ 1 & -1 & 0 & 0 & 0 \\ 0 & 1 & 0 & 0 & 0 \end{bmatrix}$

$\mathbf{B}$ = input vector = $\begin{bmatrix} 0 \\ 0 \\ \frac{2k_i A_c G P \beta_e}{V} \\ 0 \\ 0 \end{bmatrix}$

$e = \textbf{control signal} = -\mathbf{K}\,\mathbf{x} = -N\,\mathbf{K}_1\,\mathbf{K}_2\,\mathbf{x}$

$= -N\left(I_1 I_2 \dot{z}_b + J_1 J_2 \dot{z}_w + H_1 H_2 F + F_1 F_2 (z_b - z_w) + L_1 L_2 (z_w - z_r)\right)$

$\mathbf{K}$ = 1 x 5 state feedback gain vector

N = A/D gain

$\mathbf{K}_1$ = 1 x 5 state feedback gain vector for the controller

= $\begin{bmatrix} I_1 & J_1 & H_1 & F_1 & L_1 \end{bmatrix}$

$\mathbf{K}_2$ = 5 x 5 transducer gain matrix = $\begin{bmatrix} I_2 & 0 & 0 & 0 & 0 \\ 0 & J_2 & 0 & 0 & 0 \\ 0 & 0 & H_2 & 0 & 0 \\ 0 & 0 & 0 & F_2 & 0 \\ 0 & 0 & 0 & 0 & L_2 \end{bmatrix}$

$\mathbf{G}_\mathbf{d}$ = disturbance vector = $\begin{bmatrix} 0 \\ \frac{B_t}{m} \\ 0 \\ 0 \\ -1 \end{bmatrix}$

$\dot{z}_r$ = disturbance signal, i.e. velocity of road disturbance

For a regulator controller type, the disturbance term must be neglected during a controller design stage. Hence, the state equation becomes:-

$$\dot{\mathbf{x}} = \mathbf{A}\mathbf{x} + \mathbf{B}e \qquad (2)$$

Consider a full-state feedback control scheme as shown in Fig 2.

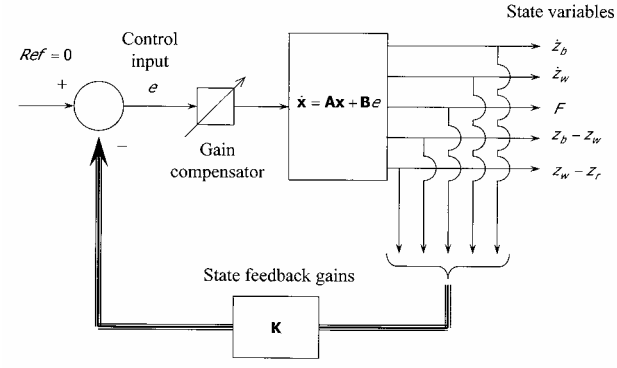

Fig 2: Block diagram of full-state feedback control

The control signal e was given by equation (1). The important question that arises is how the feedback gains of the five state variables $\mathbf{K}$ can be chosen in order to satisfy the design criterion. In this work, pole-assignment controller design was applied.

2. Pole-assignment control (PA)

The pole-assignment technique [3,11] allows the designer to specify all of the closed-loop poles. However, there is a cost associated with the placing all of the closed-loop poles, because it requires successful measurements of all state variables. There is also the requirement that the system must be completely state-controllable. This condition is used to determine whether the closed-loop poles can be placed at arbitrarily chosen locations. As mentioned, the active suspension is equivalent to the regulator control system experienced with unmeasured road input disturbances [5,18]. More specifically, it is desired to keep all of the state variables at a zero reference in the presence of disturbances. When the road input velocity and displacement are applied to the system, the state variables can be brought back to the zero reference by the controller. According to state-space model, the five state variables are: $\dot{z}_b$, $\dot{z}_w$, F , $z_b - z_w$, $z_w - z_r$, while the output variables to be controlled are: $\ddot{z}_b$, $z_w - z_b$, $z_r - z_w$.

From the motion of car body:-

$$M\ddot{z}_b = F\cos\alpha - B_v\left(\dot{z}_b - \dot{z}_w\right) \quad (3)$$

Assuming that B_v is very small [13] gives $\ddot{z}_b \propto F$. Therefore, the three variables that need to be controlled are related to a set of state variables. All of the state variables have the same dynamic closed-loop poles, which can be controlled by the pole-assignment controller.

With the power of the pole assignment technique, the closed-loop poles can be located at the specific locations in the s-plane. In general, the closed-loop poles are specified such that the system dynamic is dominated by an ideal second-order system. This allows a desired damping ratio ζ and undamped natural frequency ω_n of the dominant poles to be specified. Substituting the control signal e into equation (2) gives:-

$$\dot{\mathbf{x}} = \left(\mathbf{A} - \mathbf{BK}\right)\mathbf{x} \quad (4)$$

Stability and transient-response characteristic are determined by the eigenvalues of matrix $\mathbf{A} - \mathbf{BK}$, i.e. regulator poles. If vector $\mathbf{K}$ is chosen properly, the matrix $\mathbf{A} - \mathbf{BK}$ can be made a stable matrix. When the road inputs cause initial states shifting from the zero reference, it is possible to make $\mathbf{x}$ approach to 0 as t approaches infinity by placing the regulator poles in the left-hand of the s-plane.

Design steps can be stated as follows:-

Step 1: Check controllability condition of the system

A controllability matrix $\mathbf{M}_c$ is constructed from the system matrix $\mathbf{A}$ and the input vector $\mathbf{B}$:-

$$\mathbf{M}_c = \left[\begin{array}{ccccc} \mathbf{B} & \mathbf{AB} & \mathbf{A}^2\mathbf{B} & \mathbf{A}^3\mathbf{B} & \mathbf{A}^4\mathbf{B} \end{array}\right] \quad (5)$$

The condition for the controllability can be written in a mathematical form as:-

If $\left|\mathbf{M}_c\right| \neq \mathbf{0}$ then rank $\left[\mathbf{M}_c\right] = n$ (6)

If rank $\left[\mathbf{M}_c\right]$ is equal to n , i.e. the system order in this work, this means that there are no linearly independent column vectors in the controllability matrix. Therefore, the regulator poles of the matrix $\mathbf{A}$ can be controlled by the gain vector $\mathbf{K}$.

Step 2: Determine the coefficient terms of characteristic polynomial from matrix $\mathbf{A}$

From the characteristic polynomial for the matrix $\mathbf{A}$:-

$$\left|s\mathbf{I} - \mathbf{A}\right| = a_0 + a_1 s + a_2 s^2 + a_3 s^3 + a_4 s^4 + a_5 s^5 \quad (7)$$

determine the values of a_0, a_1, a_2, a_3, a_4 .

Step 3: Determine the transformation matrix $\mathbf{T}$ that transforms the system state equation into the control canonical form.

The matrix $\mathbf{T}$ is given by:-

$$\mathbf{T} = \mathbf{M}_c\mathbf{W}_c \quad (8)$$

where $\mathbf{M}_c$ = controllability matrix

$$\mathbf{W}_c = \begin{bmatrix} a_1 & a_2 & a_3 & a_4 & 1 \\ a_2 & a_3 & a_4 & 1 & 0 \\ a_3 & a_4 & 1 & 0 & 0 \\ a_4 & 1 & 0 & 0 & 0 \\ 1 & 0 & 0 & 0 & 0 \end{bmatrix}$$

Step 4: Specify desired closed-loop poles

The closed-loop pole locations must be chosen in such a way that the system outputs behave similar to a standard second-order system. Specifying ω_n and ζ , the closed-loop pole locations could be obtained as follows:-

$$\mu = -\sigma \pm \omega_d j \quad (9)$$

where

$$\sigma = \zeta\omega_n$$

$$\omega_d = \omega_n\sqrt{1-\zeta^2}$$

Therefore, the desired closed-loop poles for the active suspension are:-

$$\begin{aligned} \mu_1 &= -\sigma + \omega_d j \\ \mu_2 &= -\sigma - \omega_d j \\ \mu_3 &= -10\sigma \\ \mu_4 &= -10\sigma \\ \mu_5 &= -10\sigma \end{aligned} \quad (10)$$

The relationship between ω_n , ζ and the locations of the five closed-loop poles in the s-plane for the ideal second-order response is shown in Fig 3.

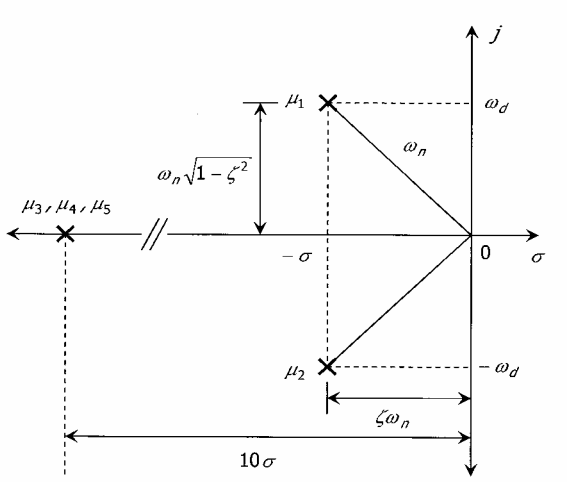

Fig 3: Locations of five closed-loop poles in the s-plane for ideal second-order responses

The μ_1 and μ_2 terms are a pair of the dominant closed-loop poles. The remaining three closed-loop poles are located far to the left of the dominant pair of the closed-loop poles and the damping of the system will be mainly caused from the dominance of the closed-loop poles. In this work, the distance, measured along the real axis, between the imaginary axis and the remaining three poles, is ten times of the distance from the imaginary axis to the dominant poles.

Step 5: Determine the coefficient terms of desired characteristic polynomial

From the desired characteristic polynomial:-

$$(s-\mu_1)(s-\mu_2)(s-\mu_3)(s-\mu_4)(s-\mu_5) = \alpha_0+\alpha_1 s+\alpha_2 s^2+\alpha_3 s^3+\alpha_4 s^4+\alpha_5 s^5 \quad (11)$$

determine the values of $\alpha_0, \alpha_1, \alpha_2, \alpha_3, \alpha_4$.

Step 6: Determine state feed back vector $\mathbf{K}$

The required state feedback gain vector can be determined from equation:-

$$\mathbf{K} = [\alpha_0 - a_0 \quad \alpha_1 - a_1 \quad \alpha_2 - a_2 \quad \alpha_3 - a_3 \quad \alpha_4 - a_4]\mathbf{T}^{-1} \quad (12)$$

From equation (4.73), the state feedback gain vector for the controller is of the form:-

$$\mathbf{K}_1 = N^{-1}\mathbf{K}\mathbf{K}_2^{-1} \quad (13)$$

From substituting constant parameters from nomenclature section, it was found that the determinant of the matrix $\mathbf{M}_c$ is equal to -7.33×10^{10}. Consequently, the rank $\mathbf{M}_c$ is 5, the system is completely state controllable. For this design example, the undamped natural frequency, ω_n = 1.56 Hz, and the damping ratio, ζ = 0.76, were used.

The desired feedback gain vector $\mathbf{K}$ is of the form:-

$$\mathbf{K} = [\alpha_0 - a_0 \quad \alpha_1 - a_1 \quad \alpha_2 - a_2 \quad \alpha_3 - a_3 \quad \alpha_4 - a_4]\ \mathbf{T}^{-1}$$
$$= [-7.56\times10^{2} \quad 2.50\times10^{3} \quad 3.59\times10^{-1} \quad 8.25\times10^{3} \quad 9.10\times10^{4}]$$

The control signal e is obtained by:-

$$e = -\mathbf{K}\mathbf{x}$$
$$= -[-7.56\times10^{2} \quad 2.50\times10^{3} \quad 3.59\times10^{-1} \quad 8.25\times10^{3} \quad 9.10\times10^{4}] \begin{bmatrix} \dot{z}_b \\ \dot{z}_w \\ F \\ z_b - z_w \\ z_w - z_r \end{bmatrix}$$

From equation (13) and N = 1600 PSCno./V, the feedback gain vector for controller $\mathbf{K}_1$ is found to be:-

$$\mathbf{K}_1 = [-9.44\times10^{-2} \quad 3.13\times10^{-1} \quad 3.37 \quad 9.01\times10^{-2} \quad 3.13]$$

he procedure for the PA design has been written in MATLAB and Control System Toolbox [9,12,16] to allow systematic designs to be processed.

3. Dynamic performance and optimum design

In order to determine the optimum design (minimum $\ddot{z}_b$ within the available $z_w - z_b$ and $z_r - z_w$), the dynamic performances of the active suspensions designed by pole-assignment control (ASPA) were investigated by simulation. The mathematical model was built up from equation (1) using SIMULINK as shown in Fig 4.

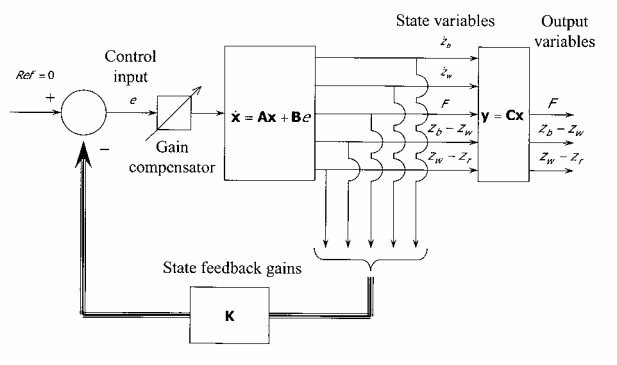

Fig 4: Simulation model representing the interaction between active suspension and road input disturbances

The details of the SIMULINK block diagram are given in Fig 5.

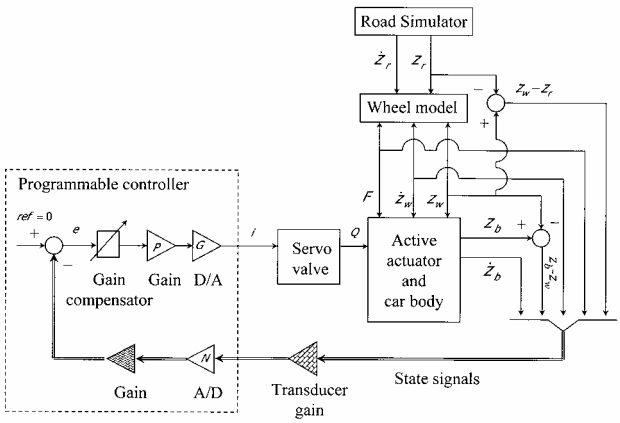

Fig 5: Simulation block diagram

According to the designs of the PA, it can be seen that it is in fact two-dimensional-search problems by tuning two parameters of interest, ω_n and ζ. The searching problems can be globalised by varying these parameters throughout the range of values of practical significance. This resulted in 150 simulation runs for each case. The random road input model [13] was used to excite the systems. The three vehicle response variables of interest ($\ddot{z}_b$, $z_w - z_b$, $z_r - z_w$) were monitored and averaged by the root mean square (rms) method. The rms $z_w - z_b$, $z_r - z_w$ were presented in the percentages of each maximum range [13]. The results of the global searching are in the form of carpet plots of $\ddot{z}_b$ vs. $z_w - z_b$ and $\ddot{z}_b$ vs. $z_r - z_w$ respectively. Therefore, a comparison between the global investigation for the passive and active suspensions can be made.

The influences of ω_n and ζ on the relationship between vibration isolation and the available $z_w - z_b$ and $z_r - z_w$ are illustrated in Fig 6-7.

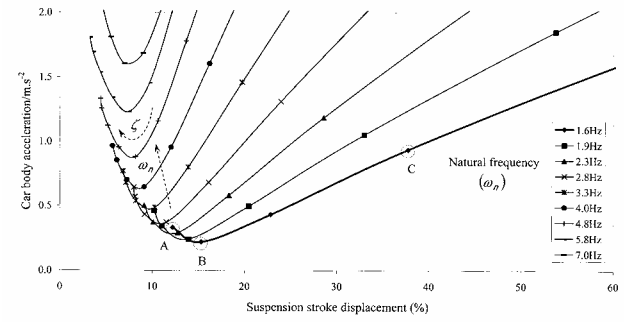

Fig 6: Relationship between rms suspension displacement and rms car body acceleration

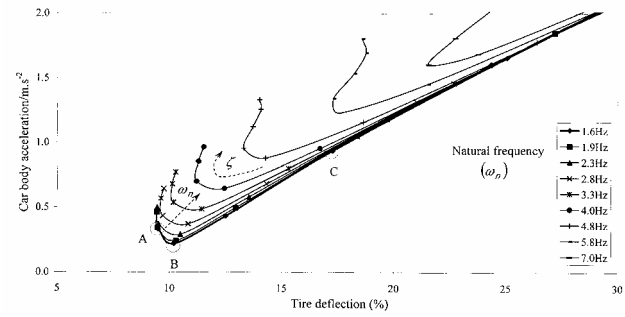

Fig 7: Relationship between rms tyre deflection and rms car body acceleration

Arrows signs are used to indicate the increments of ω_n and ζ. From the three figures, the optimum point or the minimum level of $\ddot{z}_b$ lies on the ω_n =1.6 Hz solid line ABC. Point A corresponds to a very high damping ratio (ζ = 0.94) and represents the minimum level of $z_w - z_b$ and $z_r - z_w$ at this ω_n , while point C corresponds to a lesser damping ratio (ζ = 0.50) and requires larger movement of $z_w - z_b$ and $z_r - z_w$. Point B corresponds to the minimum level of $\ddot{z}_b$ from the global searching. Therefore, point B is considered to be the optimum design of the ASPA. The design parameters at this point corresponds to ω_n =1.6 Hz and ζ =0.76. From the charts, it can be seen that the optimum ASPA is able to reduce the vibration level of the car body down to 0.22 $\mathrm{m/s^2}$ using 15% of the available $z_w - z_b$ and 10% of the available $z_r - z_w$.

4. Results and Discussions

With the advantage of the foregoing carpet plots, the optimum designs of the passive suspension (PS) developed by Surawattanawan [13] and that of the ASPA can be obtained. A comparison of the rms values of the concerned variables between both optimum designs are shown in Table 1.

Table 1: Performance comparisons between both optimum suspension designs

Concerned variables	Passive suspension (PS)	Active suspension designed by pole-assignment (ASPA)
Acceleration of car body $\ddot{z}_b$ ($\mathrm{m/s^2}$)	0.43	0.22
Suspension displacement $z_w - z_b$ (% of max. value)	17	15
Tire deflection $z_r - z_w$ (% of max. value)	10	10

It can be seen that the ASAP provides the best performance with respect to the design objective in this work, i.e. minimising the $\ddot{z}_b$. The ASPA can reduce the vibration level to 51% of that obtained from the PS whilst the ASPA utilises less suspension displacement than the PS. It is shown that the $z_w - z_b$ response in ASPA case is lower than that in PS case 12%. There is no difference for the $z_r - z_w$ responses for the both optimum designs.

The designs were finally verified by a frequency response plot, which is generated from each transfer function, containing poles and zeros information. The frequency responses relating three concerned parameters $\ddot{z}_b$, $z_w - z_b$, $z_r - z_w$ to z_r of the both optimum suspensions are compared in Fig 8-11.

The frequency response of the transfer function relating $\ddot{z}_b$ to z_r is plotted in Fig 8.

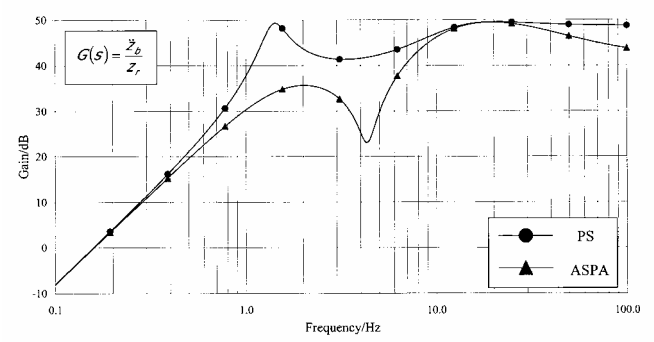

Fig 8: Comparison of the frequency response of car body acceleration for both optimum suspension designs

The optimum configuration of the PS has a relatively low damping ratio (ζ = 0.15) therefore inevitably the effect of the natural frequencies of the car body (ω_n =1.4 Hz) and that of the wheel unit (ω_n =13.6 Hz) are dominant. It can be clearly seen that the magnitude response is significantly higher at both natural frequencies. When the PA is used, it allows the dominant ω_n of the system, along with the system damping ratio to be changed. In this work, the optimum solution for the ASPA occurs for ω_n =1.6 Hz and ζ = 0.76. The magnitude response is dramatically reduced around the natural frequency of the car body and its peak is slightly shifted to a higher frequency. However, the natural frequency of the wheel unit is still dominant at the high frequency range so that it results in the increment of the magnitude around the natural frequency of the wheel unit. The frequency response of the transfer function relating $z_w - z_b$ to z_r is plotted in Fig 9.

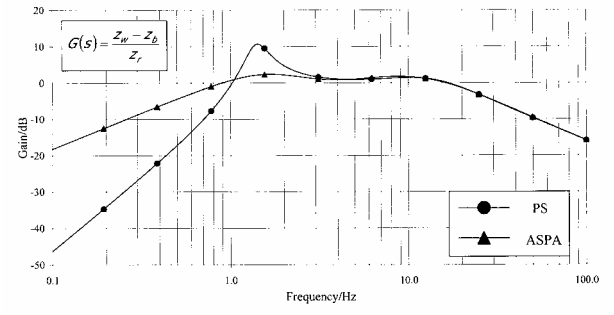

Fig 9: Comparison of the frequency response of suspension stroke for both optimum suspension designs

The $z_w - z_b$ responses of the ASPA are higher than that of the PS at the frequency lower than 1 Hz. This relationship is reversed around the natural frequency of the car body and this clearly shows the disadvantages of the PS in two aspects as follows. Firstly, the PS cannot follow the road input displacement well enough in comparison to the ASPA at the frequency lower than 1 Hz. Secondly, at the natural frequency of the car body the PS requires very large movement of $z_w - z_b$ to accommodate the resonance effect of the natural frequency. The frequency response of the transfer function relating $z_r - z_w$ to z_r is plotted in Fig 10.

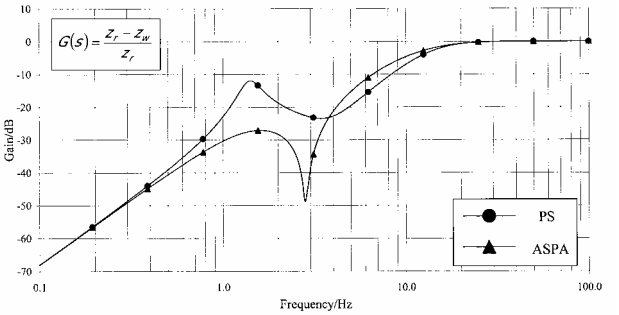

Fig 10: Comparison of the frequency response of tire deflection for both optimum suspension designs

It was found that using a logarithm scale plot for this transfer function distorts the results. Therefore, a linear scale plot is also shown in Fig 11.

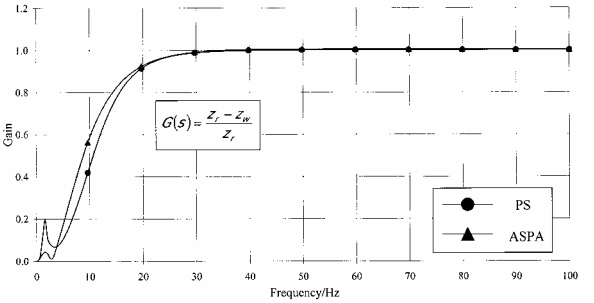

Fig 11: Comparison of the frequency response of tire deflection for both optimum suspension designs (linear scale)

Even though the $z_r - z_w$ response of the PS is the largest one among the three suspension designs at the low frequency range (around the car body ω_n), it becomes the smallest response at high frequency range. From the linear scale in Fig 11, the averages of the responses for each suspension designs are almost the same. This confirms the comparison in Table 1 that the both optimum designs utilise the same $z_r - z_w$.

5. Conclusion

The trend of carpet plots for the ASPA is similar to that of the PS. For each natural frequency, there is an optimum damping level at which the car body acceleration level is minimised. This is due to the fact that the dominant natural frequency and damping ratio in the ASPA are equivalent to the suspension stiffness and damping rate in the PS.

Even if there was no difference for the tire deflections between both optimum designs, the ASAP is superior to the PS with respect to the minimization of vibration. The ASPA can

reduce the vibration level to 51% of that obtained from the PS whilst the ASPA utilises less suspension displacement than the PS 12%.

The optimum solution of the ASPA occurs at the lowest system natural frequency. In a physical sense, the lowest system natural frequency is equivalent to the extremely soft passive suspension. The limitation of the lowest system natural frequency is the control stability. It was found that the ASPA designed by the system natural frequencies lower than 1.6 Hz will become unstable.

The large amount of damping ratio damps down the resonance around the car body natural frequency but adversely affects the transmissibility of the frequencies above the car body natural frequency. On the other hand, if the damping ratio is reduced beyond the optimum configuration, the suspension turns to be very low damping system. Transmissibility effect is reduced but the resonance due the car body natural frequency becomes more pronounced. This results in an increment of the car body acceleration. This phenomenon is similar to that in the PS case. It can be concluded that even though the ASPA provides the better performance in comparison to the PS, the conceptual designs of both are similar. The optimum designs are still the trade-off between the effects of transmissibility and system natural frequency.

References

[1] Appleyard, M. and Wellstead, P. E. Active suspensions: some background. IEE Proc.-Control Theory Appl., 1995, 142(2), pp. 123-128.

[2] Burrows, C.R. Fluid power systems - some research issues. Proc. Instn. Mech. Engrs, Part C, 2000, Vol. 214, pp. 203-220.

[3] Dorf, R. C. and Bishop, R. H. Modern control systems, 7th edition, 1995 (Addison-Wesley).

[4] Elbeheiry, E.M. et al. Advanced ground vehicle suspension systems - a classified bibliography. Vehicle System Dynamics, 1995, 24, pp. 231-258.

[5] Elbeheiry, E.M. and Karnopp, D.C., Optimal control of vehicle random vibration with constrained suspension deflection, Journal of Sound and Vibration, 1996, 189(5), pp. 547-564

[6] Engelman, G. H. and Rizzoni, G. Including the force generation process in active suspension control formulation. Proc. American Control Conference, June 1993, pp. 701-705.

[7] Hall, B. B. and Gill, K. F. Performance evaluation of motor vehicle active suspension systems. Proc. Instn. Mech. Engrs, Part D, Journal of Automobile Engineering, 1987, 201 (D2), pp. 135-148.

[8] Hrovat, D. Survey of advanced suspension developments and related optimal control applications. Automatica, 1997, Vol. 33, No. 10, pp. 1781-1817.

[9] MATLAB user's guide. The MathWorks, Inc., 2002.

[10] Mrad, R. B. et al. A nonlinear model of an automobile hydraulic active suspension system. ASME Advanced Automotive Technologies, DE-Vol. 40, 1991, pp. 347-359.

[11] Ogata, K. Modern control engineering, 3rd edition, 1997 (Prentice Hall).

[12] SIMULINK user's guide. The MathWorks, Inc., 2002.

[13] Surawattanawan, P. Mathematical modeling and analysis of automotive passive suspension, Engineering Journal Kasetsart, Vol. 47, August-November 2002, pp. 134-149

[14] Surawattanawan, P. Modeling and control of an electrohydraulic active suspension, 12th International Pacific Conference on Automotive Engineering, April 1-4, 2003, Bangkok, Thailand, pp. 1-7.

[15] Thompson, A. G. and Chaplin, P. M. Force control in electrohydraulic active suspension. Vehicle System Dynamics, 1996, 25, pp. 185-202.

[16] User's guide of control system toolbox for MATLAB, The MathWorks, Inc., 2001.

[17] Watton, J. Fluid power systems modeling, simulation, analog and microcomputer control, 1989 (Prentice Hall).

[18] Zaremba, A. et al. Optimal active suspension design using constrained optimization, Journal of Sound and Vibration, 1997, 207(3), pp. 351-364